Sub-micron machining of semiconductors - Femtosecond surface ripples on GaAs by 2 µm laser light

Mark Ramme*, Jiyeon Choi, Troy Anderson, Ilja Mingareev and Martin Richardson
Townes Laser Institute, The College of Optics and Photonics, University of Central Florida
4000, Central Florida Blvd., Orlando FL 32816-2700

ABSTRACT

In recent years, a major interest in surface as well as bulk property modification of semiconductors using laser irradiation has developed. A.Kar *et al*. [1][2] and E.Mazur *et al.* [3] have shown introduction and control of dopants by long-pulse laser irradiation and increased absorption due to femtosecond irradiation respectively. With the development of mid-IR sources, a new avenue of irradiation can be established in a spectral region where the semiconductor material is highly transparent to the laser radiation. The characterization of the light-matter-interaction in this regime is of major interest. We will present a study on GaAs and its property changes due to pulsed laser irradiation ranging from the visible to the mid-IR region of the spectrum. Long-pulse as well as ultra-short pulse radiation is used to modify the material. Parameters such as ablation threshold, radiation penetration depth and thermal diffusion will be discussed.

Keywords: Ultrashort, Laser, Mid-IR, Semiconductor, Modification, Ripples

1. INTRODUCTION

Surface structuring of various materials is a research topic of increasing interest. Bio-medical applications like directional cell growth on laminar surfaces are an example of future applications of this technique [4]. Surface-structured biocompatible substrates are necessary for the successful implementation. Chemical contamination due to the process involved can be eliminated using femtosecond 3D structuring. Another fast growing area regarding surface structuring is the improvement of photovoltaic devices. Here the studies concentrate mainly on redirecting incident light, trapping it or just increasing effective surface area and therefore increased absorption by surface structures [5][6]. Besides well-established techniques such as 2D lithography and mask mold imprinting, laser structuring is highly suitable for the requirements of new industrial applications in these topic areas. 2D lithography techniques posses inherent high cost and high maintenance facilities whereas ultrashort lasers become more powerful and cheaper every day, making even parallel processing possible. They also offer the capability of fast and easy to implement changes in the structure design, which is hardly possible with the former mentioned techniques. Furthermore, ultrashort laser processing offers new avenues of material modification that other techniques cannot fulfill due to the high field strength involved with the short pulse duration. A challenge for laser-based techniques is structuring dimensions smaller than the diffraction limit as it is given by the used radiation wavelength and focusing optics. The obvious advantages of material enhancement due to the high E-field and the immediate control have to be superior to compensate for some limitations given for direct laser structuring.

This study has investigated the generation of surface ripples, also known as laser-induced periodic surface structures (LIPSS), resulting from mid-IR femtosecond radiation. Contrary to the accepted model to LIPSS generation by longer pulse irradiation [7][8], the debate of the nature of ripple generation by ultrashort pulse radiation is still ongoing. Other researchers have reported similar observation in metals, semiconductors and dielectrics [9][10][11]. For the generation of ripples on the surface, several different models have been proposed. One model is of particular interest and states interference effects between the incident electromagnetic wave and a scattered surface wave [12]. Furthermore, some similarities to the generation of nano-spikes, as shown by Mazur *et al.* [13], can be drawn. Also, the recently shown generation of nano-gratings in bulk dielectrics is often referred to as similar effect. Two models are discussed for the bulk modification effect, on one side, interference between the incident E-field and the electron plasma wave [14], on the other side local field enhancement effect [15]. The used mid-IR radiation wavelength was chosen to allow comparison

* mramme@creol.ucf.edu; phone 1 407 823-6895; fax 1 407 823-6880; lpl.creol.ucf.edu

between the effects in dielectrics resulting in ripples as well as nano-gratings and the proposed models for their generation.

2. IRRADIATION SETUP

Two different lasers were used in this study to irradiate the samples, providing pulses with femtosecond as well as nanosecond pulse duration at the mid-IR wavelength range.

For ultrashort mid-IR irradiation, a Spectra Physics Spitfire system based on Titanium:Sapphire Kerr-mode-locked oscillator and chirped pulse amplification was used to pump an optical parametric amplifier (OPA) by Coherent (Coherent OPerA). The Spitfire system delivered fs-pulses at a wavelength of 800 nm with a pulse duration of 100 fs and a pulse energy of up to 1 mJ at 1 kHz repetition rate. The OPA provided radiation at 2 µm wavelength with pulse energies up to 40 µJ. It was assumed that the pulse duration during the conversion from 800 nm to 2 µm did not change significantly, and a measured spectrum of the mid-IR output confirmed sufficient bandwidth. In addition, the radiation from the Spitfire system could also be doubled to provide a wavelength of 400 nm and pulse energies up to 0.1 mJ. For the sample irradiation with ultrashort pulses, two tower setups were used, one optimized for high transmission at both 400 and 800 nm wavelengths, and the other optimized for high transmission at 2 µm wavelength. To simplify the alignment of the sample relative to the focusing objective, each tower setup provided sample illumination and an imaging system. In the case of the visible wavelength range, the imaging system was designed for online observation, whereas in the mid-IR tower setup, the illumination and imaging system was couple into the laser beam path via a flip-mirror and therefore only available while the laser radiation was off. The focusing optics used for the irradiation were standard white-light microscope objectives with numerical apertures (NA) of 0.25 and 0.4. The transmission of visible light ranging from 400 to 800 nm was measured to be above 80 %. On the contrary, when using these objectives with mid-IR radiation, the transmission decreased to 50 % and 66 % depending on the particular objective (refer to the table). A measurement of the focused beam diameter was performed for 2 µm radiation to gain knowledge about the actual achievable spot size. The data is shown in Figure 1.

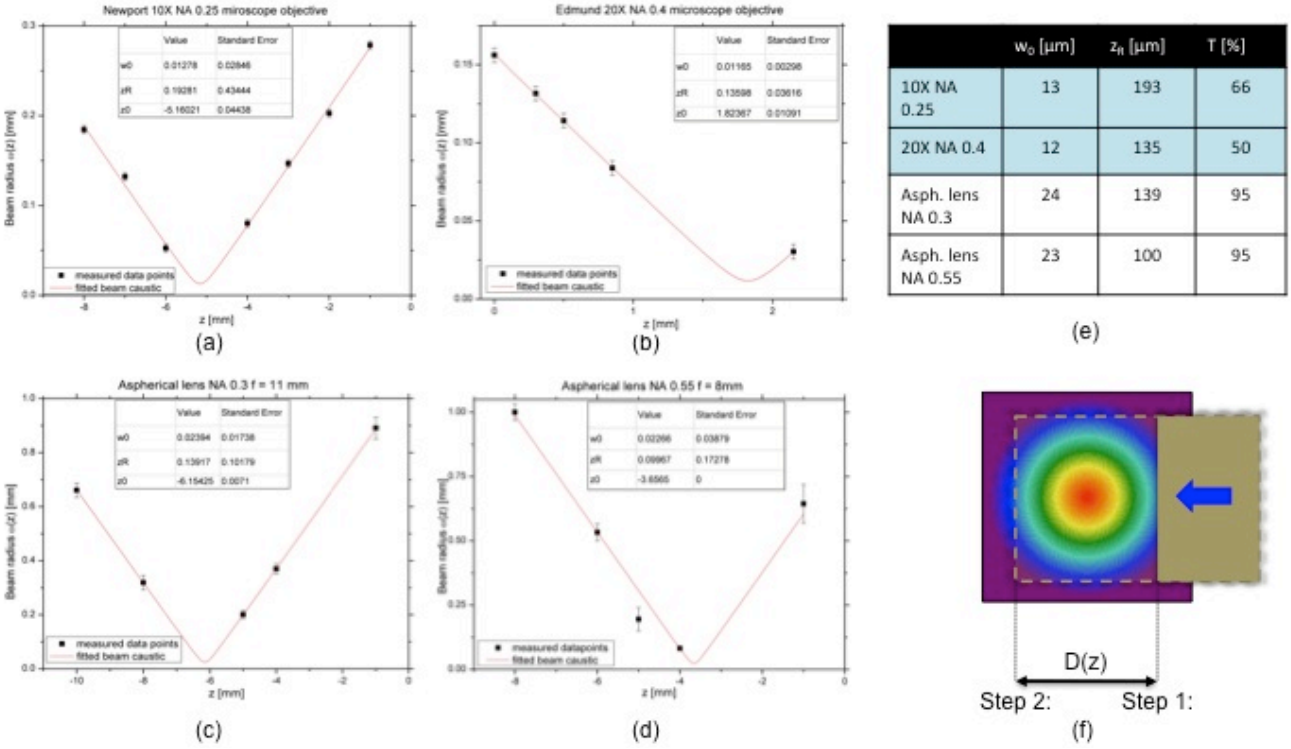

	w_0 [µm]	z_R [µm]	T [%]
10X NA 0.25	13	193	66
20X NA 0.4	12	135	50
Asph. lens NA 0.3	24	139	95
Asph. lens NA 0.55	23	100	95

Figure 1 - Measured beam caustic for used focusing optics used for 2 um radiation; (a) Newport 10X NA = 0.25, (b) Melles Griot 20X NA = 0.4, (c) aspherical lens NA = 0.3, f = 11 mm, (d) aspherical lens NA = 0.55, f = 8 mm, (e) main parameter summary of used focusing optics, (f) schema of caustic measurement for λ = 2 µm

The method of measuring the beam diameter for ultrashort radiation is shown in Figure 1 (f). The intensity distribution was measured using a mid-IR beam camera (PYROCAM III). Then a knife-edge was placed in the beam path at several z-positions. The x-position of the knife-edge was measured for the shown 2 steps, which gave the beam diameter at each z-position. A 1/e-factor was applied to allow for comparison with a Gaussian beam diameter as in the case of visible light. The apparent increase in beam waist for the 20x objective was attributed to an increase in chromatic aberrations due to the use of 2 µm radiation.The samples were mounted on a computer-controlled x,y,z-stage (Newport VP-25XA), which allowed for relative sample movement with respect to the focal spot of the incident beam. The positioning resolution of the axes is submicron with a maximal stroke of 25 mm. The stage was computer controlled and programmed using a Labview environment. An image of the materials processing setup and a scheme of the irradiation tower are shown in Figure 2.

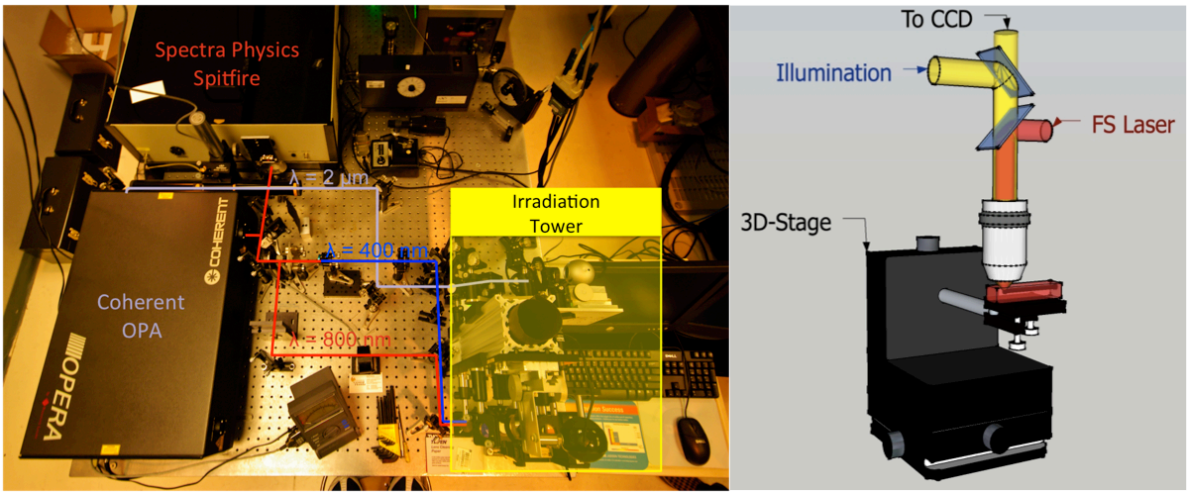

Figure 2 - Left: ultrashort irradiation station for generation of 400 nm, 800 nm and mid-IR fs-radiation, right: carton of the irradiation tower with sample illumination and imaging system

For irradiation with ns-pulsed laser radiation, an in-house developed fiber laser system based on a Thulium fiber [16] was used to deliver the 2 µm radiation at 20 kHz repetition rate and pulse energies up to 200 µJ. The pulse duration of the laser system was measured to be approximately 140 ns using a fast photo diode. The beam was focused using aspherical lenses with a NA of 0.3 and 0.55 and focal lengths of 11 mm and 8 mm, respectively. The aspherical lenses were optimized for a wavelength of 1500 nm and showed greater than 90 % transmission for the used 2 µm laser radiation. Since the beam diameter was less than the clear aperture of the used optics, the focused beam diameter was measured using a standard knife-edge scanning technique. The data is also shown in Figure 1. A computer controlled x,y,z-stage (Newport VP-25XA) was used to translate the sample with respect to the focal point.

3. SURFACE MACHINING

Intrinsic GaAs was irradiated to reduce free carrier absorption. An electronic grade GaAs wafer was used for surface modification experiments. The transmission of the material was measured using a Cary 500 spectrophotometer. The measurement was conducted on the 480 µm thick wafer sample and revealed a transmission of ~50 % over a wide spectrum from the band edge at 850 nm to a wavelength of 3 µm. It should be pointed out that the refractive index of GaAs is roughly $n \approx 3.4$ in the mid-IR region, which yields 30 % Fresnel reflection on air-GaAs interfaces.

To determine the surface modification threshold for each radiation wavelength, the beam was focused on the surface of the GaAs sample at several different pulse energies. The size of the modified region on the sample surface was measured for several pulse energies and wavelengths. A back-extrapolation was applied to estimate the modification threshold, as suggested by Lui [17]. As shown in Figure 3, the threshold for the ultrashort regime was estimated to be a few tens of mJ/cm^2. This value is about one order of magnitude lower then in the literature reported values. We have attributed this lower threshold, compared to other references, to the fact that we estimated the modification threshold from initial data taken from ablation studies. A more thorough investigation of the modification threshold including dependencies on wavelength as well as pulse duration is ongoing. In addition, measurement variances of the beam diameter are carried through as square and will also strongly contribute to the discrepancy. An estimation of the threshold at 400 nm was not

considered since the focusing spot was found to be elliptical and an estimate of squared diameter involved a large uncertainty. In the case of ns pulse duration, the modification threshold increased to 30 J/cm^2, which is three orders of magnitude greater than the modification threshold for fs pulse duration. This significant increase was attributed to a different mechanism of energy absorption in the longer pulse regime which we consider to be avalanche ionization.

After the modification threshold was determined, larger surface areas of a few square millimeters per parameter set of the GaAs wafer were irradiated. During each experiment the sample was transversally translated relative to the focal spot using various translation speeds ranging from 0.1 mm/s to 2 mm/s. For each translation speed the pulse energy was varied up to a few μJ. In addition, the radiation polarization was rotated from 0^o to 90^o with respect to the translation direction for each set of translation speed and pulse energy.

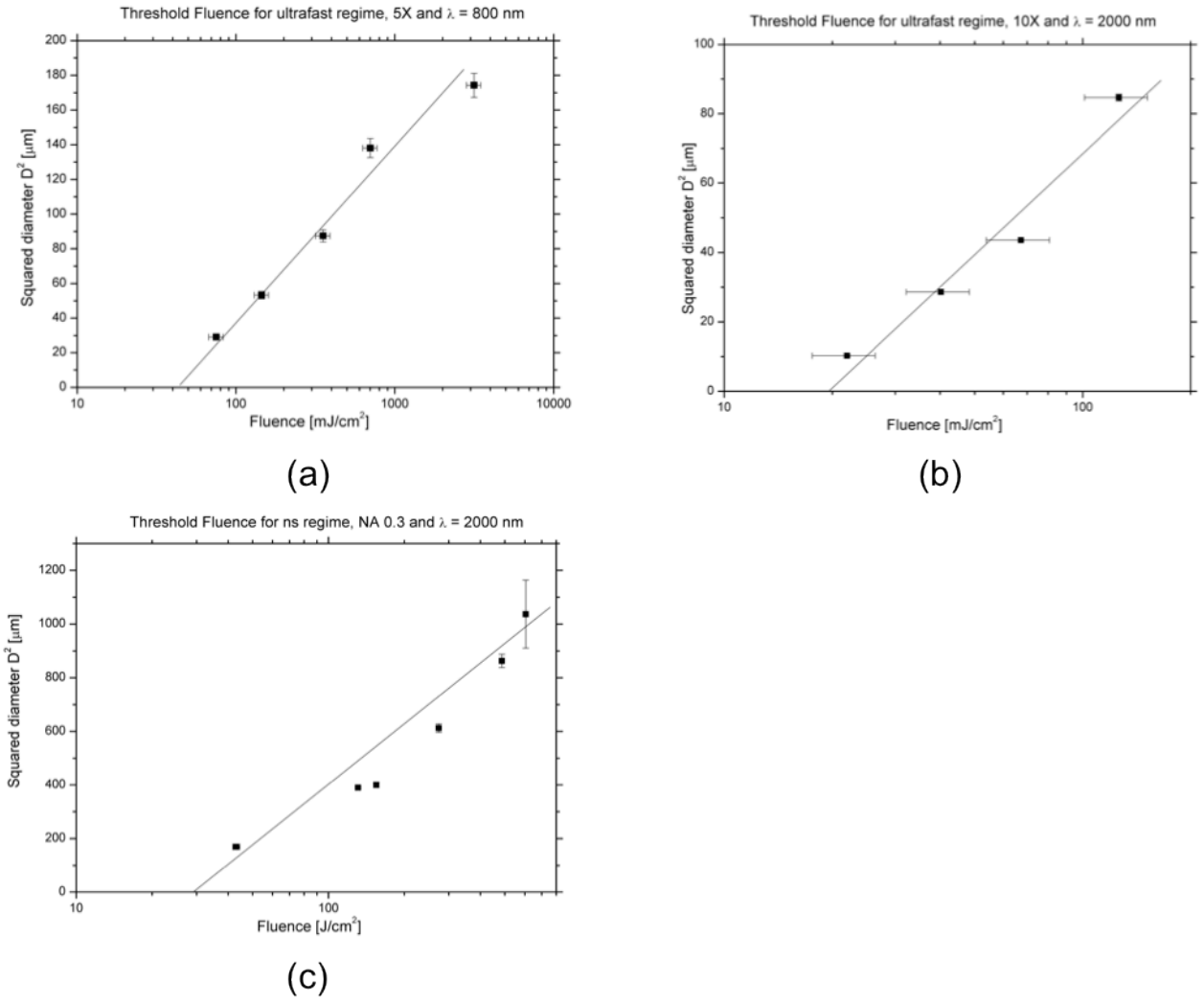

Figure 3 - Back-Extrapolation of modification threshold of GaAs using fs- and ns-pulse regime, (a) fs-regime, focused by 5X microscope objective, 800 nm wavelength; (b) fs-regime, focused by 10X microscope objective, 2000 nm wavelength; (c) ns-regime, focused by NA 0.3 aspherical lens, 2000 nm wavelength;

Using fs-laser radiation for surface modification of GaAs leads to sub-wavelength surface modification known as ripples [18]. Several features due to the incident laser radiation were found after irradiation and will be discussed hereafter.

3.1 Low spatial frequency ripple (LSFR)

The first and most prominent feature found within the irradiated area was a series of periodic grooves with a spacing of approximately the incident wavelength. Figure 4 shows the LSFR structure for incident wavelengths of 400 nm, 800nm and 2 μm and a ripple spacing Λ_{LSFR} of 500 nm, 600 nm and 1500 nm respectively.

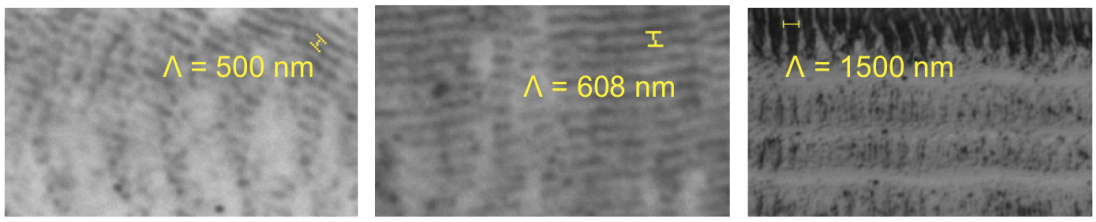

Figure 4 - LSFR spacing for different incident radiation wavelengths

Rotation of the incident radiation polarization yields a rotation of the ripples direction on the surface, as shown in Figure 5. It was found that the direction of the ripples is normal to polarization or E-field of the incident beam. Different models are proposed to describe this effect. One is that the LFSR structure is caused by interference between the incident wave and a surface wave created by the incident field [12].

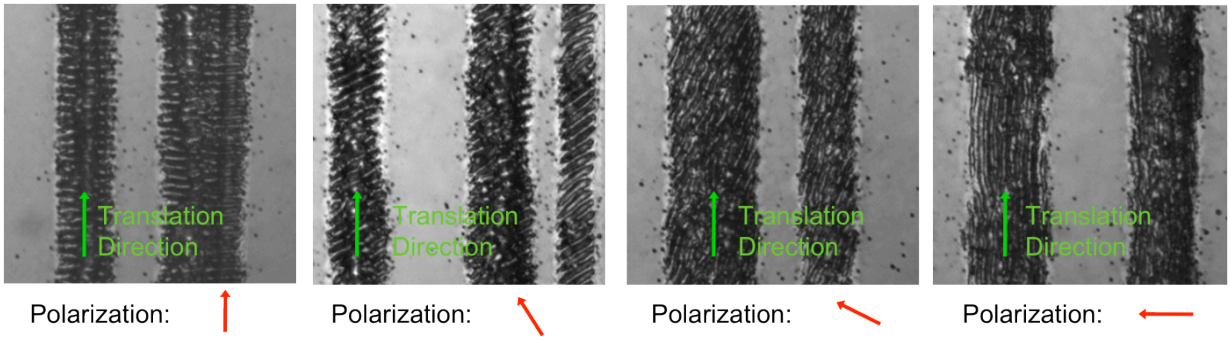

Figure 5 – Polarization dependence of high power ripples, direction of grooves changing from *s* to *p*

Furthermore, if adjacent tracks just overlap slightly, on a nanometer scale, the ripple structure is continuous and the grooves of each track line-up with the grooves of the neighboring tracks, depict in Figure 6 (a). This behavior is known as the coherent ripple effect. If the tracks are spaced apart from each other the ripples are not matched and the grooves do not necessary line-up, shown in Figure 6 (b). The reason for this memory effect is believed to be small periodic variances in the absorbance of the track surrounding material cause by the surface wave or the E-field itself. Similar phenomena were also observed when irradiating the surface of Silicon wafers.

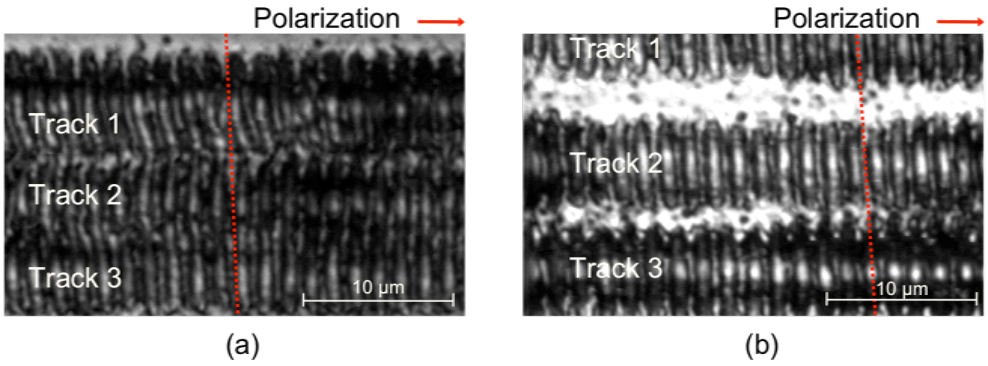

Figure 6 - (a) Continuous ripples due to overlap of the tracks; (b) Ripples are offset due to offset of 2 μm of the tracks

For pulse energies well above the ablation threshold, deep grooves were engraved in the material surface. The LSFR structure was still apparent in these grooves, as shown in Figure 7 (top).

3.2 High spatial frequency ripples (HSFR)

When the fluence level due to the incident radiation is greater then 1 J/cm^2, well above the ablation threshold of the used GaAs wafer, a second type of feature was occurring. This feature shows a much smaller ripple spacing than for the former LSFR, as depict in Figure 7. From the picture is also apparent that these features occur at the outer region of the irradiated track. The period spacing Λ_{HSFR}, here observed for an incident wavelength of 2 µm, is 300 nm and matches $\lambda/2n$ assuming a refractive index of 3.4. The explanation for higher spatial frequency could be second harmonic generation on the GaAs-air interface and an interference of E-field of this second harmonic radiation and the surface wave within the skin depth of the semiconductor. Similar effects were observed in ZnSe crystals by Jai *et al.* [19]. The orientation of the HSFR structure is the same as for the LSFR and normal to the E-field of the incident beam.

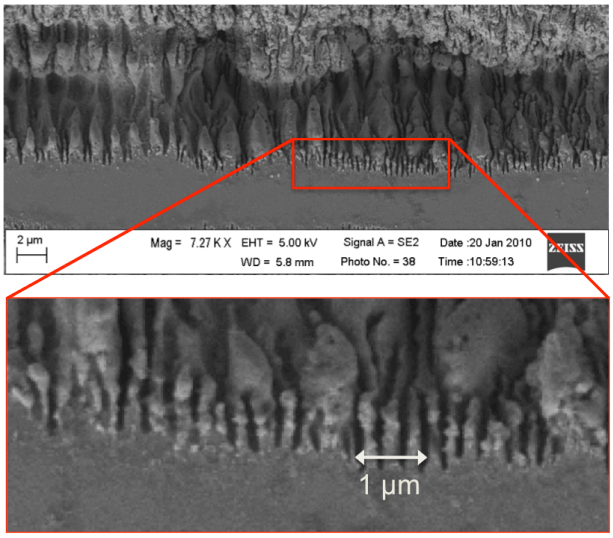

Figure 7 – Image of tracks irradiated with pulse energies well above the ablation threshold; (top) deep engraved track featuring the LSFR structure on the bottom of the track; (bottom) zoomed in view of the edge of the track, featuring the HSFR structure with a groove spacing of 300 nm

3.3 Low energy high spatial frequency ripples (LE-HSFR)

In addition to the former described features, a second periodic HSFR modification is observed when using mid-IR radiation and at low fluence levels less than 300 mJ/cm^2 as shown in Figure 8. This low-energy surface structure, here for an incident radiation wavelength of 2 µm, is characterized by a period spacing $\Lambda_{LE\text{-}HSFR}$ of approximately 500 nm and a parallel period direction with respect to the incident E-field direction. Therefore, the ripples spacing of LE-HSFR is less than observed for LSPR and greater than for HSFR structures and does not coincide with a multiple of the wavelength and refractive index. The direction of the periodicity is also normal to the former described features. The latter fact implies that interference of the incident E-field with a surface wave does not cause LSFR and HSFR here since the E-field would be parallel to the grooves. The cause for this modification is not well understood. A speculation to the cause is an imprint of the crystal orientation, even though the spacing is very large to be some sort of crystal lattice representation. More experiments are necessary and currently ongoing to give a better understanding of the underlying physical processes of this phenomenon.

This modification is only apparent at very low pulse energies and was quickly overlaid by the LSFR when the energy was increased. Therefore, this phenomenon does not scale in the same manner as LSFR structures with energy. Hence an occurrence due to material specific properties becomes more likely than an interference effect. Mazur *et.al.* showed a development of microspikes from initially laminar periodic structures [13]. Different from their finding, here no mask was used to generate the polarization-parallel ridges. It should be noted that a modulation of the energy distribution of the incident pulse could not be excluded from the list of causes for this phenomena. A further investigation of the 2 µm radiation especially in the focal region would be necessary.

Using a laser source with longer pulse durations did not lead to this type of surface modification.

4. CONCLUSIONS

Intrinsic GaAs was irradiated on the surface and coherent periodic surface modifications, known as ripples, were generated using visible and mid-IR radiation. The period of these ripples was highly correlated to the incident wavelength whereas the orientation of the periodicity was controlled by the polarization direction of the incident beam. The most prominent ripple features were low spatial frequency ripples (LSFR) with a period of approximately the incident wavelength and an orientation normal to the polarization of the incident beam. Therefore, it was shown that large areas of the material could be homogenously structured. It was further found that the translation speed has only marginal influence on the depth of the modification. The main contribution is due to the pulse energy of the incident beam. That allows for high throughput for possible applications.

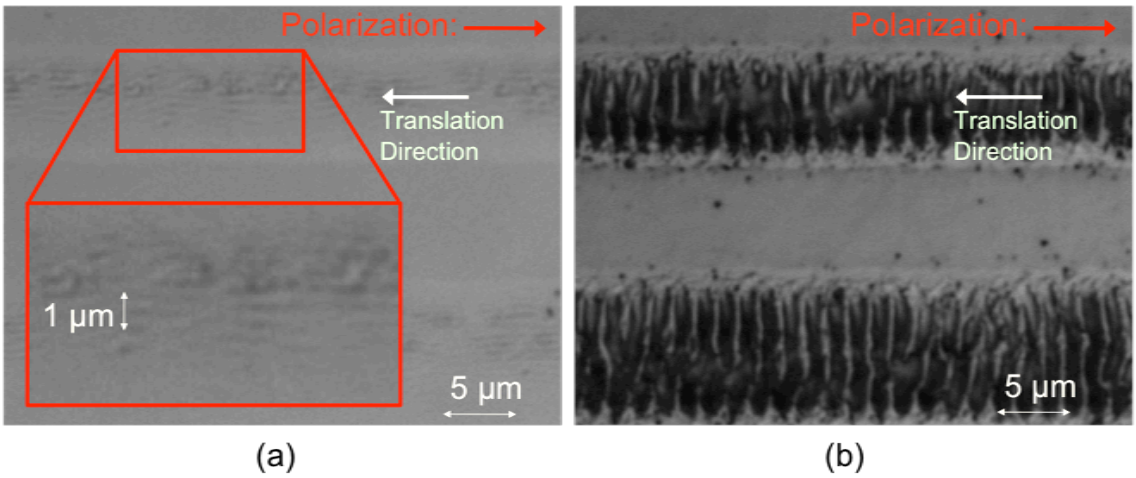

Figure 8 - Low energy HSPR (a) irradiated area with pulse energies below the modification threshold (inlay: zoomed view of one irradiation track); (b) irradiated area with pulse energies above the modification threshold

High spatial frequency ripples (HSFR) were generated using mid-IR radiation at a wavelength of 2 µm. The period of the HSFR was measured to $\lambda/2n$ and the orientation was coincidental with the orientation of the LSFR. The features were generated on the edges of deep ablation tracks when using greater pulse energies above the ablation threshold of the material.

Irradiating the GaAs surface with very low fluences (less than 300 mJ/cm^2) led to a third type of ripples, oriented 90^o to the direction of the former L/HSFL structures. This ripple structure vanishes due to the overlaid LSFR at higher fluences.

With the presented research it was shown that control of the period spacing could be realized over a wide range from beyond the diffraction limit at sub-micron distances to several micrometer depending on the available radiation source. With the additional control of the direction of the periodicity and the high coherence of the generated structures this technique enables new applications in bioengineering and electronics. Nevertheless, the on-going research will investigate the involved physical mechanism further to gain a better understanding of the underlying light-matter interaction processes and their influences on material properties.

5. REFERENCES

[1] S Bet, N Quick, A Kar, “Laser-doping of silicon carbide for p-n junction and LED fabrication,” Phys Status Solidi A vol. 204 (4) 1147-1157(2007)

[2] S Bet, N Quick, A Kar, “Laser doping of chromium as a double acceptor in silicon carbide with reduced crystalline damage and nearly all dopants in activated state,” Acta Mater vol. 56 (8) 1857-1867 (2008)

[3] MA Sheehy, BR Tull, CM Friend, E Mazur “Chalcogen doping of silicon via intense femtosecond-laser irradiation,” Mat Sci Eng B-Solid vol. 137 (1-3) 289-294 (2007)

[4] E Martinez, E Engel, J. A Planell, J Samitier, “Effects of artificial micro- and nano-structured surfaces on cell behaviour,” Ann Anat vol. 191 (1) 126-135 (2009)
[5] A Halbwax, T Sarnet, Ph Delaporte, A Sentis, H Etienne, F Torregrosa, V Vervisch, I Perichaud, S Martinuzzi, “Micro and nano-structuration of silicon by femtosecond laser: Application to silicon photovoltaic cells fabrication,” Thin Solid Films vol. 516 (20) 6791-6795 (2008)
[6] C.H Crouch, J.E Carey, M Shen, Eric Mazur, F Genin, “Infrared absorption by sulfur-doped silicon formed by femtosecond laser irradiation,” Appl Phys A vol. 79 (7) 7 (2004)
[7] JE Sipe, JF Young, JS Preston, HM Van Driel, “Laser-induced periodic surface-structures - 1. Theory,” Phys. Rev. B vol. 27 (2) 1141-1154 (1983)
[8] AM Bonch-Bruevich, MN Libenson, VS Makin, VV Trubaev, “Surface electromagnetic-waves in optics,” Opt Eng vol. 31 (4) 718-730 (1992)
[9] J Gottmann, G Schlaghecken, R Wagner, E Kreutz, “Fabrication of erbium-doped planar waveguides by pulsed-laser deposition and laser micromachining,” Proc. SPIE (2003)
[10] Q Sun, F Liang, R Vallee, SL Chin, “Nanograting formation on the surface of silica glass by scanning focused femtosecond laser pulses,” Opt. Lett. vol. 33 (22) 2713-2715 (2008)
[11] Juergen Reif, Olga Varlamova, Florenta Costache, “Femtosecond laser induced nanostructure formation: self-organization control parameters,” Appl Phys A vol. 92 (4) 1019-1024 (2008)
[12] M Couillard, A Borowiec, H. K Haugen, J. S Preston, E. M Griswold, G. A Botton, “Subsurface modifications in indium phosphide induced by single and multiple femtosecond laser pulses: A study on the formation of periodic ripples,” J Appl Phys vol. 101 (3) pp. 033519 (2007)
[13] M Shen, C Crouch, J Carey, R Younkin, E Mazur, “Formation of regular arrays of silicon microspikes by femtosecond laser irradiation through a mask,” Appl. Phys. Lett. vol. 82 (11) (2003)
[14] Y Shimotsuma, M Sakakura, S Kanehira, J Qiu, P G Kazansky, K Miura, K Fujita, K Hirao, “Three-dimensional Nanostructuring of Transparent Materials by the Femtosecond Laser Irradiation,” Journal of Laser Micro/Nanoengineering,” vol. 1 (3) 181 (2006)
[15] VR Bhardwaj, E Simova, PP Rajeev, C Hnatovsky, RS Taylor, DM Rayner, PB Corkum, “Optically produced arrays of planar nanostructures inside fused silica,” Phys Rev Lett vol. 96 (5) 057404 (2006)
[16] CCC Willis, L Shah, M Baudelet, TS McComb, RA Sims, V Sudesh, MC Richardson, “High-energy Q-switched m3+-doped polarization maintaining silica fiber laser”, paper 7580-2 to be published in Photonics West 2010, Proc. SPIE 7580 (2010)
[17] JM Liu, “Simple technique for measurements of pulsed Gaussian-beam spot sizes,” Optics Letters, Vol. 7, Issue 5, 196-198 (1981)
[18] A Borowiec, M MacKenzie, GC Weatherly, HK Haugen, “Femtosecond laser pulse ablation of GaAs and InP: studies utilizing scanning and transmission electron microscopy,” Appl Phys A-Mater vol. 77 (3-4) 411-417 (2003)
[19] TQ Jia, HX Chen, M Huang, FL Zhao, JR Qiu, RX Li, ZZ Xu, XK He, J Zhang, H Kuroda, “Formation of nanogratings on the surface of a ZnSe crystal irradiated by femtosecond laser pulses,” Phys. Rev. B vol. 72 (12) 125429 (2005)